Published in final edited form as:
Dev Dyn. 2009 September ; 238(9): 2292–2308. doi:10.1002/dvdy.22036.

CELL AUTONOMOUS REQUIREMENTS FOR *DLG-1* FOR LENS EPITHELIAL CELL STRUCTURE AND FIBER CELL MORPHOGENESIS

Charlene Rivera[1,†,§], **Idella F. Yamben**[1,†], **Shalini Shatadal**[1], **Malinda Waldof**[1], **Michael L. Robinson**[2], and **Anne E. Griep**[1,*]

[1]Department of Anatomy University of Wisconsin School of Medicine and Public Health Madison, WI 53706

[2]Department of Zoology Miami University Oxford, OH 45056

Abstract

Cell polarity and adhesion are thought to be key determinants in organismal development. In *Drosophila*, *discs large* (*dlg*) has emerged as an important regulator of epithelial cell proliferation, adhesion and polarity. Herein, we investigated the role of the mouse homolog of *dlg* (*Dlg-1*) in the development of the mouse ocular lens. Tissue specific ablation of *Dlg-1* throughout the lens early in lens development led to an expansion and disorganization of the epithelium that correlated with changes in the distribution of adhesion and polarity factors. In the fiber cells differentiation defects were observed. These included alterations in cell structure and the disposition of cell adhesion/cytoskeletal factors, delay in denucleation, and reduced levels of α-catenin, pERK1/2 and MIP26. These fiber cell defects were recapitulated when *Dlg-1* was disrupted only in fiber cells. These results suggest that *Dlg-1* acts in a cell autonomous manner to regulate epithelial cell structure and fiber cell differentiation.

Keywords

Dlg-1; PDZ; lens development; mouse; cell adhesion; cell polarity; cytoskeleton

INTRODUCTION

Cell polarity and adhesion are thought to be key determinants in organismal development and cell proliferation and differentiation. In *Drosophila*, the tumor suppressor, *discs-large* (*dlg)* has been shown to be a crucial regulator of these processes (Woods et al., 1996; Bilder and Perrimon, 2000). In this study, we address the importance of *Dlg-1*, the mouse homolog of *Drosophila dlg*, in the development of the mouse ocular lens.

The mouse ocular lens is an ideal developmental model for understanding how cell polarity and adhesion are modulated *in vivo* and how these affect tissue development. Being composed entirely of epithelial cells, it is a relatively simple organ that is part of a more complex organ system, the eye. The morphological features of lens development are well characterized. Lens formation starts with the induction of the head ectoderm into the lens

[*]Corresponding Author: Dr. Anne E. Griep Department of Anatomy University of Wisconsin School of Medicine and Public Health 1300 University Avenue Madison, WI 53706 Ph: 608-262-8988/FAX: 608-262-7306 aegriep@wisc.edu.
[†]These authors contributed equally to this work.
[§]Present address: Lineberger Comprehensive Cancer Center University of North Carolina Chapel Hill, NC 27599

placode by the underlying optic cup at around embryonic day 9.5 (E9.5) and its subsequent invagination to form the lens vesicle by day E10.5. Shortly thereafter, cells in the posterior half of the lens vesicle undergo terminal differentiation into lens fiber cells during which they elongate to fill the vesicle, completely occluding the vesicle by day E13.5 (Piatigorsky, 1981). At this point, the lens consists of a mass of differentiated fiber cells that is bordered on its anterior surface by a monolayer of epithelium. The lens continues to grow by the continual addition of newly differentiating cells from the epithelium to the fiber cell compartment. By the time of birth, within the epithelium, cells in the anterior region are mostly quiescent, whereas cells in the peripheral region, referred to as the germinative zone, are actively dividing. As cells divide, they migrate, or are displaced, posteriorly into the transition zone, where they permanently withdraw from the cell cycle and differentiate into fiber cells. As they differentiate, fiber cells become highly elongated, express lens specific differentiation markers, including β and γ crystallins, MIP26 and filensin, and eventually lose all membrane-bound organelles (Piatigorsky, 1981). In this fashion, the lens continues to grow throughout the life of an organism, albeit at a slower rate as the animal ages, due at least in part to the slower rate of proliferation in the epithelium (Piatigorsky, 1981).

Many factors are known to be involved in the development of the lens. Among these are the pRb pocket proteins family (Morgenbesser et al., 1994; Pan and Griep, 1994), multiple growth factor signaling pathways such as FGF, IGF-1, TGFα, BMP and Wnt (reviewed in (Lovicu and McAvoy, 2005), and cell adhesion proteins including α6 integrin (Walker et al., 2002), β1 integrin (Simirskii et al., 2007) and E- and N-cadherin (Ferreira-Cornwell et al., 2000; Pontoriero et al., 2008). Although our knowledge of individual factors that contribute to the regulation of lens proliferation and differentiation is extensive, it remains unclear how these factors are coordinated to ensure proper regulation of lens growth and differentiation.

(**P**SD-95-**D**lg-**Z**O-1) domain-containing proteins (PDZ proteins) contain a common protein-protein recognition domain of approximately 80-90 amino acids (Harris and Lim, 2001). PDZ proteins, through their multiple protein-protein interaction domains (including the PDZ domain), are thought to act as scaffolding molecules capable of assembling large macromolecular signaling complexes at the cell membrane. In invertebrates such as *Drosophila melanogaster* and *Caenorhabditis elegans*, two PDZ domain proteins, Discs large (Dlg) and Scribble (Scrib), have been shown to play a role in positioning and maintaining the components of adherens junctions and apical determinants, which is critical for cell-cell adhesion (Woods et al., 1996; Bilder et al., 2000; Bilder and Perrimon, 2000; Bossinger et al., 2001; Firestein and Rongo, 2001; Koppen et al., 2001; McMahon et al., 2001; Segbert et al., 2004). In *Drosophila*, mutations in *dlg* or *scrib* result in the ectopic localization of adherens junctions and apical proteins in various epithelial tissues, including the embryonic epidermis, the imaginal disc, and the follicular epithelium. Epithelial cells in these *Drosophila* mutants loose their columnar cell shape and are found disorganized in a multilayered epithelium. Due to these characteristics, *dlg* and *scrib* have been classified as neoplastic tumor suppressors in this organism (Woods and Bryant, 1989; Woods et al., 1996; Bilder et al., 2000; Bilder and Perrimon, 2000).

Recently, we have gathered evidence in support of the hypothesis that PDZ domain-containing proteins are critical factors in the regulation of lens cell growth and differentiation. Dlg-1, Scrib and numerous other PDZ proteins are expressed throughout the ocular lens (Nguyen et al., 2003). Dlg-1 and Scrib show co-localization with each other and with the cell adhesion proteins E-cadherin, N-cadherin, and the apical protein ZO-1 (Nguyen et al., 2005). Dlg-1 was highly concentrated in the apical regions of the fiber cells, as was N-cadherin, (Nguyen et al., 2005) where the zonula adherens is located (Lo et al., 2000; Zampighi et al., 2000), and at the basal tips of fiber cells (Nguyen et al., 2005) where the basal membrane complex is found (Bassnett et al., 1999). Expression in the mouse lens of

the E6 oncoprotein from Human papillomavirus type 16 (HPV-16), which binds to and inactivates multiple PDZ proteins including Dlg (Kiyono et al., 1997; Glaunsinger et al., 2000; Nakagawa and Huibregtse, 2000; Thomas et al., 2002), resulted in the disorganization and hyperproliferation of the lens epithelium, as well as the inhibition of lens fiber cell differentiation (Pan and Griep, 1994; Nguyen et al., 2002; Nguyen et al., 2003); and this property of E6 correlated with its ability to bind to and inactivate PDZ proteins including Dlg-1 (Nguyen et al., 2003)(Yamben and Griep, unpublished observations). The altered pattern of proliferating cells as well as an increase in the total numbers of cells in the lens epithelium of mice carrying an insertional mutation in *Dlg-1* (Caruana and Bernstein, 2001; Nguyen et al., 2003), further suggest that Dlg-1 may play an important role in proper lens development.

The HPV E6 transgenic mice do not provide us the ability to distinguish between effects on Dlg-1 versus other PDZ proteins targeted by E6, nor do they allow us to examine epithelial phenotypes that would arise during embryogenesis, as the K14 driven HPV transgenes are only expressed postnatally in the lens. Additionally, phenotypes observed in the Dlg gene trap mutant mice need to be considered with some reservation, as Dlg^{gt} allele still contains three intact PDZ domains (Caruana and Bernstein, 2001) and, therefore, may not be a null allele. To understand if Dlg-1 specifically is required in lens development, and, if so, what role it plays, we assessed the effects of the conditional deletion of *Dlg-1* in the mouse lens. The conditional deletion of *Dlg-1* at the lens vesicle stage resulted in multiple defects in both the epithelial and fiber cell compartments, including defects in cell cycle regulation, differentiation, adhesion and polarity. In contrast, conditional deletion of *Dlg-1* specifically in lens fiber cells recapitulated the fiber cell defects only, indicating that the effects of the loss of *Dlg-1* in these cells were direct. These results show that *Dlg-1* is required for multiple aspects of lens development in an epithelial and fiber cell autonomous manner.

RESULTS

Generation of *Dlg-1* conditional null mice

To study the role of *Dlg-1* in lens development, we generated mice carrying a *Dlg-1* conditional null allele. As shown in Fig. 1A a tri-lox targeting vector (V) was engineered and introduced into ES cells (see Experimental Procedures for details). Correctly targeted clones were used to generate chimeric mice; the chimeras were bred to C57BL/6J mice, and germ line transmission was confirmed by Southern blot and PCR analysis. To remove the neo cassette, mice carrying the targeted allele (T) were mated to *EIIA-Cre* transgenic mice, and male F1 progeny containing all possible recombination events, as judged by PCR screening of tail DNA, were mated to stock mice. Tail DNAs from the F2 progeny were genotyped by PCR to identify mice carrying the fully recombined (null) allele or the partially recombined, (floxed, F) allele. Mice carrying the null allele showed lens defects; however, due to the severe craniofacial defects these mice exhibited, it was not possible to determine if the lens defects were lens autonomous (Rivera, et al. manuscript in preparation).

To conditionally delete *Dlg-1* in the mouse ocular lens, mice containing the floxed *Dlg-1* allele were mated to mice expressing Cre under the control of a chimeric promoter containing the 32bp Pax6 consensus binding site fused to the murine *aA crystallin* promoter (referred to as *MLR10* mice) (Zhao et al., 2004). In *MLR10* mice, expression of cre begins around embryonic day 10.5 (E10.5) at the lens vesicle stage of lens development and cre expression is found throughout the lens, in both epithelial and fiber cells. Additionally, to delete *Dlg-1* specifically in fiber cells, *Dlg-1* floxed mice were mated to mice expressing cre under the control of the *aA crystallin* promoter (referred to as *MLR39* mice), which

expresses cre only in the fiber cells beginning at day E12.5 in embryogenesis (Zhao et al., 2004).

To demonstrate that cre-mediated deletion had occurred specifically in the lens, genomic DNA was prepared for PCR analysis from the lenses of neonatal *Dlg-1*$^{f/f}$ and *Dlg-1*$^{f/f}$*;MLR10* mice (hereafter referred to as *Dlg10* mice), the rest of the eye of *Dlg10* mice, and the fiber cells of *Dlg-1*$^{f/+}$ and *Dlg*$^{f/f}$*;MLR39* mice (hereafter referred to as *Dlg39* mice). As shown in Fig. 1B, cre-mediated deletion of exon 8 was evident in the DNAs from the lenses of *Dlg10* and *Dlg39* mice, but not in the DNA from the eye of *Dlg10* mice. Protein lysates were prepared from the lenses of control, *Dlg10* and *Dlg39* mice, as well as from lung of E18.5 *Dlg-1*$^{+/+}$ and *Dlg-1*$^{-/-}$ embryos. The lysates were subjected to western blot analysis with an anti-Dlg-1 antibody and subsequently the membranes were reblotted for GAPDH as a loading control. The levels of Dlg-1 in the lenses of *Dlg*$^{f/+}$10 were reduced when compared to *Dlg-1*$^{+/+}$ lenses, and undetectable in the lenses of *Dlg10* mice (Fig. IC). Also, the levels of Dlg-1 were reduced in a gene dosage dependent manner in the lenses from *Dlg*$^{f/+}$*39* and *Dlg39* mice. No Dlg-1 was detected in the protein lysate of E18.5 *Dlg-1*$^{-/-}$ lung, indicating the specificity of the antibody. Together, these results indicate that cre mediated deletion of *Dlg-1* in the lens was efficient.

Effect of loss of *Dlg-1* on lens morphology

To determine if the conditional deletion of *Dlg-1* in the lens resulted in morphological defects, embryonic day 13.5 (E13.5) embryos, E17.5 eyes, postnatal day 2 (P2) eyes and adult eyes from *Dlg-1*$^{+/+}$, *Dlg-1*$^{f/f}$, *Dlg10* and *Dlg39* mice were embedded in paraffin, sectioned, stained with hematoxylin and eosin and viewed by light microscopy. The lens phenotype of the *Dlg-1*$^{f/f}$ mice was indistinguishable from that of *Dlg-1*$^{+/+}$ mice (data not shown) and therefore, lenses from mice of these genotypes were used interchangeably for controls. In *Dlg-1*-sufficient controls, the central epithelium had the expected monolayered organization with the cells attaining a cuboidal shape over time (Figs. 2C, 2H, 3D). Abnormalities in the epithelial compartment of the lenses from the *Dlg10* embryos were observed as early as E13.5; at which time the central epithelium was thickened and areas of disorganization including regions of multilayering (Fig. 2D, boxes) were present, giving the appearance of more cells in the epithelium. To determine if this was the case, we counted the total number of cells in the epithelium of control and *Dlg10* mice at E13.5. As shown in Fig. 4, the number of epithelial cells in the lenses from E13.5 embryos was significantly greater than the number in the controls (154.1+/−0.44 vs. 108.8+/−3.26, $p<0.05$). At E17.5, in the central epithelium irregularities in the shape, staining characteristics, and the arrangement of the nuclei within the epithelial layer were observed (compare Figs. 2H and 2I, boxed regions). Regions of multilayering were observed, particularly in the peripheral regions of the epithelium (not shown). The total epithelial cell number was greater in the lenses of *Dlg10* embryos as compared to controls (202.8+/−3.6 vs. 169.1+/−2.8, $p<0.01$). By P2, the integrity of the epithelium was severely disrupted. The central epithelium in lenses of *Dlg10* mice appeared flattened as compared to the central epithelium in the control lenses and the normal uniform positioning of nuclei within the cells was lost (Figs. 3D, E). Loosely packed cells, clusters of nuclei followed by gaps in the row of nuclei (Fig. 3E, box) and vacuoles (Fig. 3E, arrow) were observed. A few areas of multilayering were observed in the peripheral epithelium (data not shown). At P2, there was no significant difference in epithelial cell numbers (209.6+/−7.61 vs. 210+/−9.13, $p=0.71$). By P24, a few areas of multilayering and the irregularities in shape of the nuclei in the peripheral epithelium of the *Dlg10* mice were still observed (Fig. 3N, arrows) and the central epithelium remained flattened as compared to controls (data not shown). These epithelial defects were not observed in the lenses of *Dlg39* mice (Figs. 2J, 3F) indicating that the *Dlg10* phenotypes were due to the loss of *Dlg-1* specifically in the epithelium.

A prominent feature of mouse lens fiber cell morphology is the positioning of the nuclei within the fiber cells through interkinetic nuclear migration (Zwaan et al., 1969). This results in the organization of the fiber cell nuclei in a pattern referred to as the bow shape, which is located parallel to the lens equator (Zwaan et al., 1969). The lenses from the control mice, most prominently at E17.5, exhibited the characteristic bow shape organization of nuclei within the fiber cell compartment (Figs. 2E, 2K, 3G, 2K). In contrast, the bow regions of *Dlg10* and *Dlg39* fibers were irregularly organized (Figs. 2F, 2G, 2L, 2M, 3I, 3L). Nuclei were positioned posterior to the bow (Fig. 2L, box) or the characteristic bow shape was completely absent (Fig. 3I, Box). Additionally, in the lenses of postnatal *Dlg-1* mutant mice, nuclei were observed in regions of the fiber cell compartment that normally are devoid of nuclei (Figs. 3G-I, arrows, 3K-L), suggesting that the denucleation process was delayed.

Secondary fiber cell differentiation includes the elongation and migration of cells along their posterior and anterior surfaces towards the center of the lens (Piatigorsky, 1981). As a part of this process, the curvature of the fiber cells switches from concave to convex so that the tips of the cells face toward the center of the lens. As fiber cells from either half of the lens approach the center, they detach from their anterior and posterior surfaces and form new connections with other fiber cells from either half of the lens resulting in the formation of anterior and posterior lens sutures. In the lenses of the *Dlg-1* sufficient control mice, sutures formed normally and fiber cells exhibited a convex curvature and (Figs. 2E, K). In contrast, in the lenses of *Dlg10* and *Dlg39* mice, defects in both anterior and posterior suture formation were observed frequently at E17.5 and P2 (Figs. 2F, 2G, 3B, 3C, asterisk). Furthermore, fiber cells in the lenses of the *Dlg10* and *Dlg39* mice in some cases failed to exhibit convex curvature (Figs. 2L, M) and in other cases had an irregular curvature (Fig 3I). The irregularity in fiber cell curvature may also contribute to the abnormal shape of the lenses and shortened anterior-posterior dimension, which was frequently observed in both *Dlg39* (Fig. 3C) and *Dlg10* (data not shown) mice. Finally, fiber cells in the lenses of *Dlg10* and *Dlg39* P2 mice appeared to stain more lightly with eosin than did the corresponding cells in the lenses of the control mice (Figs. 3C, 3I vs. 3A, 3G). Collectively, the morphological defects in the lenses of the *Dlg10* mice resulted in a cataractous adult lens (Fig. 3J). Lenses from adult *Dlg39* mice also exhibited cataracts (not shown). Together, these data suggest individual roles for *Dlg-1* in maintaining cell morphology in the epithelium and in the fiber cell compartment that is required for lens clarity.

Effect of loss of *Dlg-1* on cell survival

Disruption of fiber cell differentiation in the lens is associated frequently with apoptosis (Yan et al., 2006). To determine if the ablation of *Dlg-1* resulted in apoptosis, TUNEL assays were performed on paraffin embedded eye sections of E17.5 and P2 control, *Dlg10* and *Dlg39* mice. At E17.5, lenses from control, *Dlg10* and *Dlg39* mice showed only an occasional apoptotic cell within the epithelium (Fig. 5A-C, arrow in B), which is a normal occurrence (Ishizaki et al., 1998; Zandy et al., 2005). However, one out of 7 *Dlg* mutant lenses tested showed some TUNEL positive nuclei in the fiber cell compartment (data not shown), suggesting that cell death due to loss of *Dlg-1* may initiate around E17.5 or soon thereafter. By P2, the frequency of TUNEL positive cells in the epithelium of *Dlg10* mice was greater than in the epithelium of the control lenses (compare Fig. 5G-H and J-K, arrows in H and K) and this appeared to be an epithelial cell specific effect as there was no increase in the number of TUNEL positive cells in the epithelium of *Dlg39* mice (Fig. 5I, L). In the fiber cell compartment, no TUNEL positive cells were observed in the center of the lens or in the newly differentiating fiber cells in the cortical region in the lenses of control mice (Fig. 5G, J), as by P2 the denucleation process has already been completed. In contrast, TUNEL positive cells were observed in the center of the lenses of P2 *Dlg10* and *Dlg39* mice (Fig. 5H and K, I and L, respectively, arrows), suggesting a delay in denucleation.

Additionally, mislocalized propidium iodide (PI) positive nuclei were observed in the posterior and center in lenses of the *Dlg10* and *Dlg39* mice (Fig. 5H-I, arrowheads). Thus, loss of *Dlg-1* resulted in a temporally dependent onset of apoptosis in both epithelial and fiber cell compartments. Additionally, cell death in one compartment was independent of cell death in the other compartment.

Analysis by hematoxylin and eosin staining suggested that the organization of nuclei in the bow region was affected in lenses of the *Dlg10* and *Dlg39* mice (Figs. 2, 3). The propidium iodide staining used in the TUNEL assay also showed that nuclei were found in the anterior and posterior regions of the fiber cell compartment in the lenses of the *Dlg10* and *Dlg39* mice whereas these regions were clear of nuclei in lenses of control mice (see arrowheads in 5B, C, H and I). By P2, the overall organization of the bow region was disrupted in lenses of the *Dlg-1* mutant mice and the density of nuclei in newly differentiating fibers in the lenses of *Dlg10* mice (Fig. 5D, E boxed regions) appeared to be greater than in controls. Because fiber cell differentiation involves the proper organization and eventual loss of fiber cell nuclei, these observations suggest that fiber cell differentiation is disrupted when *Dlg-1* is ablated in the lens. Furthermore, because these structural defects are observed temporally before cell death occurs, cell death is likely the result of defects in fiber cell differentiation rather than the cause.

Effect of loss of *Dlg-1* on fiber cell differentiation

The process of fiber cell differentiation is accompanied by upregulation of differentiation specific markers. To determine if loss of *Dlg-1* affected the expression of proteins associated with fiber differentiation, eye sections from day P2 control, *Dlg10* and *Dlg39* embryos were subjected to immunofluorescence with antibodies for β-crystallin and MIP26, two fiber cell specific proteins (Graw, 1997; Chepelinsky, 2003), and phosphorylated ERK (pERK), a membrane associate protein kinase which has been shown to be upregulated in newly differentiating fibers (Lovicu and McAvoy, 2001). There was no apparent difference in the pattern of immunostaining for MIP26 and β-crystallin in the lenses of the *Dlg10* or *Dlg39* mice as compared to control lenses (Fig. 6G-L). However, the pattern and intensity of immunostaining for pERK1/2 was reduced in the newly differentiating fiber cells in the lenses of *Dlg10* and *Dlg39* mice, as compared to controls (Fig. 6D-F, boxes), suggesting that the normal upregulation in levels of the differentiation marker, activated pERK, had failed to occur (Fig. 6A-F). Additionally, patchy staining was observed, suggesting that the distribution of pERK in the fibers was affected (Fig. 6F, box). To further evaluate the effect of loss of *Dlg-1* on MIP26, β-crystallin and pERK levels, pooled protein lysates of fiber cells dissected from lenses of P2 control and *Dlg39* mice were subjected to immunoblot analysis using antibodies against total ERK1/2, activated, phosphoERK1/2 (p-ERK1/2), MIP26, β-crystallins, and GAPDH as a loading control. Whereas the levels of total ERK1 and ERK2 were similar in fiber cell extracts from *Dlg39* mice as compared to control extracts, the levels of pERK1 and pERK2 in *Dlg39* extracts were reduced (Fig. 7). Levels of MIP26 were reduced, although not to the same degree as pERK1/2. (Fig. 7) whereas the overall levels of β-crystallins were similar to controls (not shown). These data correlate structural defects in fiber cell differentiation in the *Dlg-1* mutant mice with biochemical data showing reduced levels and altered distribution of an intermediate signaling factor known to be upregulated during fiber cell differentiation.

Effect of loss of *Dlg-1* on the cell adhesion factors and cytoskeletal structure

The cell adhesion factors, E- and N- cadherin, have been shown recently to be essential for fiber cell differentiation and for maintaining normal lens epithelial structure and adhesion in the mouse (Pontoriero et al., 2008). Additionally, functional N-cadherin-actin cytoskeletal linkages are necessary for differentiation of chick lens epithelial cells into fiber cells *in vitro*

(Ferreira-Cornwell et al., 2000). Previously, we have shown that Dlg-1 co-localizes with the adherens junction proteins E- and N-cadherin in the lenses of postnatal mice (Nguyen et al., 2005) and with α-catenin, one factor linking cadherin to the actin cytoskeleton (Rivera et al., in preparation). Therefore, we asked if disruption in cell structure and fiber cell differentiation observed in the lenses of *Dlg10* and *Dlg39* mice were associated with changes in cadherin-catenin linkages and organization of the actin cytoskeleton.

To determine if the conditional deletion of *Dlg-1* in the lens affected the co-localization of E- or N-cadherin with α-catenin, longitudinally oriented paraffin sections from lenses of E17.5 and P2 control, *Dlg10* and *Dlg39* mice were double immunostained with antibodies against E- or N-cadherin and α-catenin and the sections viewed by confocal microscopy. In lenses from control mice, E-cadherin strongly co-localized with α-catenin on the basal membranes of the epithelial cells (Fig. 8A, arrow). E-cadherin was strongly concentrated on the basal membrane and in specific punctate pattern on the apical surface (Fig. 8D, arrows). In contrast, the co-localization of E-cadherin with α-catenin was lost in the lens epithelium of the *Dlg10* mice (Fig. 8B). E-cadherin was more uniformly distributed around the membranes of epithelial cells (Fig. 8B, E, arrows) and the punctate pattern of staining on the apical surface was lost (Fig. 8E). The effect of loss of *Dlg-1* on the co-localization of E-cadherin and α-catenin and the pattern of E-cadherin localization was specific to the lenses of *Dlg10* mice, as the normal pattern of localization was preserved in the epithelium of the *Dlg39* mice (Fig. 8C, F).

In lenses from the control mice, N-cadherin strongly co-localized with α-catenin at the epithelial-fiber interface, lateral membranes and posterior tips of the fiber cells in the transition zone (Fig. 9A, C arrows). In contrast, in the lenses of the *Dlg10* and *Dlg39* mice, the co-localization between N-cadherin and α-catenin was reduced (Fig. 9B, D). In control lenses α-catenin accumulated strongly at the basal tips of the fiber cells and was highly associated with the membrane in the posterior portions of the cortical fibers (Fig. 9E, G, arrows). In lenses from *Dlg10* and *Dlg39* mice, however, the accumulation of α-catenin at the basal tips of the fiber cells and the overall intensity of staining appeared to be reduced (Figs. 9F, H, arrows). The analysis of α-catenin localization by immunofluoresence suggested that the overall levels of α–catenin may be reduced in the newly differentiating fiber cells. Immunoblotting of whole cell protein lysates from fiber cells of *Dlg39* mice with antibodies against α–catenin and GAPDH, as a loading control, confirmed this possibility (Fig. 7). Finally, as noted above, as fiber cells begin to differentiate, they normally reorient themselves along the lens capsule, and take on a convex curvature. This reorientation is highlighted by the staining of N-cadherin along the membranes and basal tips of the fiber cells in control lenses (Figs. 9I, yellow arrowheads). In contrast, the basal tips of the fiber cells in the *Dlg10* and *Dlg39* mice appeared randomly oriented with respect to the capsule (Figs. 9J, K, yellow arrowheads).

The pattern of immunostaining for N-cadherin and α-catenin on longitudinal sections of control and *Dlg-1* mutant lenses suggested that the co-localization of these proteins in the transition zone was disrupted with the loss of *Dlg-1*. To further address this possibility, transverse sections of lenses from control and *Dlg39* mice were double immunostained with anti-N-cadherin and anti-α-catenin antibodies. In lenses from control mice, the hexagonal shape of the fiber cells just posterior to the transition zone was apparent (Fig. 10A-C). N-cadherin and α-catenin strongly co-localized at the vertices of the fiber cells (Fig. 10A, arrow) and on the short sides of the fibers, where N-cadherin is concentrated (Fig. 10C). Additionally, α-catenin accumulated strongly at the basal tips of the fibers where they associated with the lens capsule (Fig. 10B, asterisk). In contrast, the regular hexagonal shape of the fiber cells was lost in the lenses of the *Dlg39* mice (Fig. 10D-F). The co-localization of α-catenin and N-cadherin also was affected. The punctate accumulation of these proteins

at the vertices was lost. In some fibers, these proteins appeared to overlap along the entire membrane whereas in other fibers, they overlapped on only a portion of the membrane (Fig. 10D, arrows). The accumulation of α-catenin at the basal tips was reduced (Fig. 10B, asterisk, 10E). The disruption in cell shape and pattern of co-localization of α-catenin and N-cadherin in the lenses of the *Dlg39* mice suggested that the association of α-catenin with β-actin might also be affected. To address this possibility, transverse sections were double immunostained with anti-α-catenin and anti-β actin antibodies. In control lenses these proteins strongly co-localized at the vertices (Fig. 10G, arrow) where β-actin is concentrated (Fig. 10I, arrow). In contrast, this co-localization was lost in the fiber cells of the Dlg39 mice (Fig. 10J). In some cells, β-actin and α-catenin staining was observed along the entire membrane; however, overlap was absent or sporadic (Fig. 10J-L, arrows). Together these data indicate that loss of *Dlg-1* leads to changes in the distribution and levels of factors involved in cell adhesion that correlate with defects in fiber cell structure.

The disruption in the pattern of β-actin immunostaining and loss of the normal hexagonal shape of the fiber cells suggested that there may be defects in the organization of the underlying actin cytoskeleton. To determine if this was the case, frozen sections from lenses of P2 control *Dlg10 and Dlg39* mice were stained with phalloidin to visualize filamentous actin and analyzed by confocal microscopy. In the lenses of the control mice, actin filaments were highly organized and staining was very strong at the apical (Fig. 11A, arrow, 11D) and basal tips (not shown) of the fiber cells. In contrast, in the lenses of the *Dlg10 and Dlg39* mice, actin staining appeared highly disorganized. The intensity of staining at the apical tips of the fiber cells frequently appeared to be reduced (Fig. 11 C, box) and suture defects were apparent (Fig. 11B, C, asterisks). Interestingly, actin organization in the epithelium appeared unaffected by loss of *Dlg-1* (Fig. 11D, E). Taken together, these results indicate that the deletion of *Dlg-1* in the lens is sufficient to affect the organization the actin cytoskeleton in a fiber cell autonomous manner.

Effect of loss of *Dlg-1* on the localization of ZO-1

The PDZ protein ZO-1 is specifically localized to the apical membrane in the epithelial cells of the lens, although it is widely distributed in the fiber cells (Nielsen et al., 2003; Nguyen et al., 2005). To determine if the conditional deletion of *Dlg-1* in the lens vesicle affected apical-basal polarity, longitudinally oriented paraffin sections from lenses of day E17.5 control and *Dlg10* mice were immunostained with anti-ZO-1 antibody and the sections viewed by confocal microscopy. In the central epithelium, ZO-1 localization was restricted to the apical membranes of epithelial cells in lenses from control mice (Fig. 12A, arrow). By contrast, ZO-1 was observed on all membranes of the central epithelial cells from the *Dlg10* mice (Fig. 12B). Interestingly, in the transition zone, ZO-1 remained restricted to the apical surface of the epithelial cells in the lenses from the *Dlg10* mice (Fig. 12E). In addition, ZO-1 distribution in the central fiber cells appeared more diffuse in lenses from the *Dlg10* mice (Fig. 12B) as compared to controls (Fig. 12A). Localization of ZO-1 in the epithelium of lenses from *Dlg39* mice was indistinguishable from ZO-1 staining in control mice (Figs. 12C, F). Thus, this result suggests that apical-basal polarity is affected in specific regions of the epithelium when *Dlg-1* is ablated in the lens and that this effect is epithelial cell autonomous.

DISCUSSION

Cell polarity and adhesion are thought to be key determinants in organismal development and in the maintenance of epithelial structure and tissue architecture. In this study, we addressed the hypothesis that *Dlg-1* is required for regulating these essential aspects of epithelial cell biology during the development of the mouse ocular lens. We show that loss of *Dlg-1* specifically affects epithelial cell integrity, growth and survival. Independently,

loss of *Dlg-1* affects fiber cell structure, differentiation and survival. We show that these defects correlate with defects in cell adhesion, cytoskeletal organization, and apical-basal polarity factors. Finally, we show that the loss of *Dlg-1* leads to reduced levels of α-catenin, MIP26 and activated pERK1/2, factors that are essential for maintaining normal cell architecture and fiber cell differentiation. Thus, we provide evidence that *Dlg-1* is required for multiple independent aspects of lens formation in an epithelial and fiber autonomous manner.

Dlg-1 is required for maintaining the structural integrity of the epithelium

By conditionally targeting deletion of *Dlg-1* in the lens as early as E10.5, we found that loss of *Dlg-1* by day E13.5 resulted in a disorganized epithelium characterized by irregular cell shape and positioning, areas of multilayering, and an increase in total cells (Figs. 2, 3, and 4). One possible explanation for the multilayering is that there may be defects in the orientation of cell division, which was occasionally observed (data not shown). Although multilayering could contribute to the disorganized appearance of the epithelium, the vast majority of the epithelium is not multilayered (Figs. 2 and 3); and therefore, additional factors, are likely to be involved. Prior studies have suggested that Dlg is a negative regulator of G1/S phase transition (Ishidate et al., 2000;Brumby et al., 2004;Nagasaka et al., 2006). Furthermore, lenses of day E19.5 $Dlg^{gt/gt}$ embryos showed increased total epithelial cell number and proliferating cells in the transition zone (Nguyen et al., 2003). Therefore, altered cell cycle regulation in the lens epithelium of *Dlg10* embryos prior to E13.5 may contribute to the increased total number of cells in the epithelium at day E13.5 and 17.5. However, as by P2 there was no disparity in epithelial cell number between *Dlg10* mice and controls (Fig. 4), any effect that loss of *Dlg-1* in the epithelium might have on cell cycle regulation is temporally regulated. The increased number of TUNEL positive cells in the epithelium at this age suggests that apoptosis is involved (Fig. 5). However, apoptosis may only be one factor since the increase in TUNEL positive cells was small. Further studies will be required to elucidate the role of *Dlg-1* in cell cycle regulation in the epithelium.

One additional factor that could contribute to the irregularities in cell shape and disorganization of the epithelium might be the defects of apical-basal cell polarity. Studies in *Drosophila* indicate that Dlg is required for proper apical-basal polarity and the formation and maintenance of adherens junctions (Bilder et al., 2003). In our study, we found that the tight junction protein and polarity marker ZO-1 was no longer restricted to punctate regions on the apical surfaces of the central epithelial cells in the lenses of the *Dlg10* mice; instead, ZO-1 was also observed along the basolateral surfaces (Fig. 12). Of note, tight junctions are found only in the central epithelium in the lens (Lo et al., 2000; Zampighi et al., 2000) and, therefore, tight junctions may be compromised in the *Dlg-1* deficient epithelium. Another factor that could contribute to irregularities in cell shape in the epithelium might be the defects in cell-cell adhesion. Previous mammalian cell culture studies have shown that Dlg-1 localizes to sites of cell-cell adhesion (Reuver and Garner, 1998). In our study, we observed that the normal distribution of E-cadherin in the epithelial cell membranes and its overlap with α-catenin was disrupted in the epithelium of *Dlg10* mice (Fig. 8), suggesting that loss of *Dlg-1* in these cells resulted in defects in cell-cell adhesion. Thus, loss of *Dlg-1* in the lens alters the distribution and levels of polarity and adhesion factors, suggesting that Dlg-1 is required for the formation and/or maintenance of apical-basal polarity and adherens junctions in the lens.

In our study we have identified the first in vivo example of a requirement for *Dlg-1* to properly localize polarity factors such as ZO-1 and adhesion factors such as E-cadherin. Interestingly, changes in ZO-1 or E-cadherin distribution were not observed in the urogenital tract defects in $Dlg^{gt/gt}$ (Naim et al., 2005) or *Dlg-1* null (Iizuka-Kogo et al., 2007) mice. Thus, the loss of *Dlg-1* has tissue specific effects on cell polarity and adhesion in the mouse.

One possible explanation for this difference is that in the urogenital tract other factors such as other Dlg family members may have redundant roles and/or can compensate for the loss of *Dlg-1*.

Dlg-1 is required in fiber cells for cell structure and differentiation

In both the *Dlg10* and *Dlg39* models, loss of *Dlg-1* resulted in multiple defects in fiber cell morphology including defects in the organization of the bow region, fiber cell elongation and suture defects, loosely packed fibers and vacuoles, and defects in the concave curvature of the fibers (Figs.2 and 3). In addition, TUNEL positive nuclei were retained in the lens nucleus (Fig. 5H, I, K, L), suggesting, at least, a delay in the denucleation program. The fact that these same phenotypes were observed in the fiber cell specific *Dlg39* model indicates that *Dlg-1* plays a fiber cell autonomous role in lens development. Furthermore, the observation that TUNEL positive nuclei were observed in the cortical fibers only at P2 (Fig. 5H, I, K, L) whereas defects in differentiation were already apparent at E17.5 (Figs. 2E-I, 6A-F), may suggest that these defects accumulated over time and eventually become severe enough to trigger apoptosis. Alternatively, there may be temporally dependent signals required to trigger apoptosis in the lenses of the *Dlg10* and *Dlg39* mice.

The morphology and movement of fiber cells are greatly dependent on the plasticity of cell-cell adhesion, cell-matrix adhesions and the interaction of these adhesions with the underlying cytoskeleton (Zelenka, 2004). In particular, N-cadherin is required for fiber cell differentiation (Pontoriero et al., 2008) and linkages involving N-cadherin (Ferreira-Cornwell et al., 2000) and the actin cytoskeleton (Maddala et al., 2008) have been shown to be important in this process. We have shown previously that Dlg-1 is highly concentrated in the apical and basal tips of the fiber cells, where it strongly co-localizes with N-cadherin (Nguyen et al., 2005). In this study, we showed that the morphological abnormalities observed in the lenses of the *Dlg10* and *Dlg39* mice (Figs. 2 and 3) were associated with a disruption in the overlap between N-cadherin and α-catenin (Figs. 9A-D, 10A-F) and α-catenin and β-actin (Fig. 10G-L) in cortical fiber cells. Additionally, the organization of the actin cytoskeleton (Fig. 11) was disrupted, particularly in the apical regions of the fiber cells, which may result from a disruption of the zonula adherens, a region where Dlg-1 is normally found to be highly concentrated and to strongly co-localize with N-cadherin (Nguyen et al., 2005). At the basal capsule, the accumulation of α-catenin (Fig. 10B, E) and regular organization of the fiber cell tips with respect to the lens capsule was affected (Figs. 9I-K). Taken together, the data indicate that *Dlg-1* deficiency may lead to the observed structural defects in the fiber cells because of defects in cell adhesion-cytoskeletal linkages. Defects in fiber cell elongation, abnormal accumulation of nuclei in the transition zone, disorganization of the actin cytoskeleton and extensive vacuolization of fiber cells have been observed in the lenses of mice conditionally ablated for *Cdh2 (N-cadherin)* (Pontoriero et al., 2008). These similarities in the phenotypes of the *Dlg-1* deficient and *Cdh2* deficient lenses support the hypothesis that Dlg-1 is a modulator of N-cadherin function.

Interestingly, α-catenin staining appeared to be reduced in the fiber cells of the *Dlg10* and *Dlg39* mice (Figs. 9E-G, 10B, E), an observation that was confirmed by immunoblot analysis using fiber cell protein extracts from *Dlg39* mutants (Fig. 7). To our knowledge, a role for *Dlg-1* in maintaining α-catenin levels has not been previously reported. The pronounced disorganization of the actin cytoskeleton may be a consequence of the reduced level of α-catenin and aberrations in the signaling pathways that are associated with cytoskeletal organization. It has recently been shown that increased concentrations of α-catenin allow for this molecule to homodimerize resulting in its ability to interact with actin filaments (Drees et al., 2005). Cytoskeletal organization also has been shown to be compromised when RhoGTPase activity is inhibited in the fiber cells (Maddala et al., 2008).

Future studies will be required to elucidate the mechanism through which loss of *Dlg-1* results in reduced α-catenin levels and disorganization of the actin cytoskeleton.

Dlg-1 as a modulator of ERK1/2 activation

In our study, we tested the effect of loss of *Dlg-1* on the expression of the lens fiber cell differentiation markers β crystallin, MIP26 (Graw, 1997; Chepelinsky, 2003) and the upregulation in the levels of pERK1/2 (Lovicu and McAvoy, 2001). We observed no apparent change in the level or pattern of β-crystallin expression (Figs. 6J-L and data not shown). This is consistent with previous reports showing by immunofluorescence that upregulation of β-crystallin during fiber cell differentiation is pERK1/2 independent (Lovicu and McAvoy, 2001), We also observed a small reduction in MIP26 (Fig. 7), although the pattern of MIP26 expression was not affected (Fig. 6G-I). Reduced MIP26 is consistent with the findings of Golestaneh et al. (Golestaneh et al., 2004) who found that pharmacologically inhibiting ERK activity in the rat explant system resulted in reduced MIP26 expression. Interestingly, we found that the levels of pERK1/2 appeared to be reduced in the newly differentiating fiber cells of both *Dlg10* and *Dlg39* mice (Fig. 6A-F). Analysis of fiber cell extracts from *Dlg39* mice confirmed that levels of pERK1/2 were reduced, whereas the levels of total ERK1/2 were unaffected (Fig. 7). This is the first report suggesting a role for *Dlg-1* in regulating ERK activation.

One explanation for the reduced levels of pERK1/2 with the loss of *Dlg-1* is that cell adhesion (Figs. 7, 9, 10) and the actin cytoskeleton are disrupted (Fig. 11). In keeping with Dlg-1's role as a scaffolding molecule, associated with this disruption is the failure to assemble the correct protein complexes for efficient ERK phosphorylation. Scaffolding proteins have been shown to be necessary to correctly localize ERK1/2 to the protein complexes for phosphorylation (Ramos, 2008). One known protein is the scaffolding and actin binding molecule, IQGAP1, which can bind several members of the ERK1/2 pathway and can activate ERK1/2 in response to growth factor stimulus (Brandt and Grosse, 2007;Ramos, 2008).

Another possible explanation for reduced levels of pERK1/2 in the *Dlg-1* deficient fiber cells is that Dlg-1 modulates growth factor signaling pathways that impact fiber cell differentiation through ERK activation. It has been established that FGF signaling is necessary for fiber cell differentiation (McAvoy and Chamberlain, 1989; Chow et al., 1995; Robinson et al., 1995; Lovicu and Overbeek, 1998; Robinson et al., 1998; Stolen and Griep, 2000; Zhao et al., 2008) and that FGF induced differentiation requires sustained pulses of pERK1/2 activity (Iyengar et al., 2007). Other growth factor signaling pathways such as BMP (Faber et al., 2002), TGFβ (de Iongh et al., 2001; Faber et al., 2002), integrin (Walker et al., 2002; Simirskii et al., 2007) and noncanonical Wnt signaling (Chen et al., 2004; Chen et al., 2006; Chen et al., 2008) also are known to influence fiber cell differentiation and these signaling pathways have been linked to upregulation of pERK1/2 (Walker et al., 2002; Golestaneh et al., 2004; Lyu and Joo, 2004; Iyengar et al., 2007). Similarities in the lens phenotypes of mice in which the FGF (Chow et al., 1995; Robinson et al., 1995; Stolen and Griep, 2000), Wnt (Chen et al., 2008), and integrin (Walker et al., 2002) pathways are inhibited suggest these may be plausible targets for Dlg-1. Further experiments are needed to determine which pathway or pathways and signaling cascades are modulated by *Dlg-1* in the lens.

Conclusions

Dlg-1 is required in both the epithelium and the fiber cell compartment for regulating epithelial structure and fiber cell differentiation and may do so, at least in part, through the regulation of cell polarity, cell-cell adhesion and cytoskeletal organization. Our findings also

describe novel roles for *Dlg-1* in maintaining α-catenin and MIP26 levels and pERK1/2 activation, which are essential for maintaining normal cell architecture and fiber cell differentiation.

EXPERIMENTAL PROCEDURES

Animal Maintenance and Use

All experiments using mice conformed to the Public Health Service Policy on Humane Care and Use of Laboratory Animals and ARVO statement for the Use of Animals in Ophthalmic and Vision Research and were approved by the Institutional Animal Care and Use Committee of the University of Wisconsin School of Medicine and Public Health.

Generation of *Dlg-1* Mutant Mice

A 7.1kB fragment encoding exons 7-9 of *Dlg-1* was isolated from a murine strain 129/Sv CITB BAC library and used to generate the targeting vector via recombineering (Liu et al. 2003) (see Figure 1A). The linearized vector was electroporated into R1 embryonic stem (ES) cells and ES cells containing the integrated vector were identified by Southern Blot analysis. Three karyotypically normal clones containing the targeted allele were microinjected into C57BL/6J blastocysts. The resulting chimeras were bred to C57BL/6J mice and agouti progeny were tested for germline transmission of the mutant allele by Southern Blot analysis of tail DNA and by PCR. The construction of the targeting vector, generation of gene targeted ES cell clones and generation of chimeric mice were carried out in the University of Wisconsin Biotechnology Center's Transgenic Animal Facility.

Female *Dlg-1*$^{fn/+}$ mice were mated to male *EIIAcre* transgenic mice (Lakso et al 1999) and the F1 mosaic progeny were mated to C57Bl/6J, 129X1SvJ or FVB/nJ females and mice with the conditional allele (*Dlg-1*$^{f/+}$ mice) or null allele (*Dlg-1*$^{+/-}$ mice) were identified by PCR screening Dlg 5′ and Dlg-1 I8R (conditional allele) or Dlg 5′ and Dlg-1 3′ (Table 1). To conditionally delete *Dlg-1* in the lens, first *Dlg-1*$^{f/+}$ mice were mated to either homozygous *MLR10* or homozygous *MLR39* mice (Zhao 2004). Progeny containing the floxed allele were identified using Dlg 5′ and DlgI8R primers. Progeny containing cre were identified by PCR using Pr4 and creAS (Zhao et al., 2004). Next, *Dlg-1*$^{f/+}$*;MLR10* and *Dlg-1*$^{f/+}$*;MLR39* progeny were mated to *Dlg-1*$^{f/+}$ mice. To confirm lens specific cre mediated deletion, genomic DNA isolated from microdissected lenses, lens fibers, the rest of the eye and tail was subjected to PCR amplification using Dlg5′ and Dlg3′ primers.

Western Blotting

Whole lenses or fiber cells were dissected from P2 and neonatal lenses and protein was isolated using 1X RIPA buffer with protease inhibitors. 100μg of protein lysate from *Dlg-1*$^{+/+}$, *Dlg*$^{f/f}$, *Dlg* $^{f/+}$*10*, *Dlg10* or *Dlg*$^{f/+}$*39*, *Dlg39* mice were run on a 7.5% acrylamide gel. Lung protein extracts from *Dlg-1*$^{+/+}$ and *Dlg-1*$^{-/-}$ were also prepared and used as controls (Fig. 1C). Proteins were transferred to PVDF membrane. Blots were blocked in 5% nonfat dry milk dissolved in 1X phosphate buffered saline-tween 20 (PBST) or 5% bovine serum albumin (BSA) in tris buffered saline-tween 20 (TBST), for pERK1/2. Membranes were probed for three hours with the antibodies and concentrations listed in Table 2 diluted in blocking solution. Membranes were washed in 1X PBST or 1X TBST and were then incubated for one hour with goat anti-mouse HRP (Pierce) or donkey anti-rabbit HRP (GE Healthcare Life Sciences) diluted in blocking solution. After incubation with the secondary antibodies, blots were washed and bands were visualized using Enhanced Chemiluminescence Plus Kit (ECL Plus, GE Healthcare Lifesciences) and exposed to film or scanned on a StormScanner densitometer. As a loading control, blots were incubated with

mouse anti-GAPDH diluted in blocking solution, washed, and then were incubated with goat anti-mouse HRP.

Histological Analysis

Embryos from E13.5 and eyes from day E17.5, P2 and P24 *Dlg-1*$^{+/+}$, *Dlg-1*$^{f/f}$, *Dlg10* and *Dlg39* mice were dissected and fixed overnight in 4% paraformaldehyde (PFA) at 4°C, washed with 1X phosphate buffered saline (PBS) and dehydrated in increasing concentrations of ethanol. Embryos were oriented for coronal sectioning and eyes were oriented for either longitudinal or transverse sectioning. Both were embedded in paraffin. 5μm sections were cut, stained with hematoxylin and eosin, and viewed by light microscopy. The total cell number in the epithelium was determined by counting nuclei under a light microscope at 40X magnification. At least 3 animals per genotype per age and 2 slides per animal per age were used. Statistical significance was determined by the Wilcoxon Rank Sums test (two-sided) and $p<0.05$ was considered statistically significant. To assess lens clarity, lenses from control and *Dlg10* mice were viewed under a dissecting microscope.

Determination of Apoptosis

Day E17.5 and P2 eyes from *Dlg-1*$^{+/+}$, *Dlg-1*$^{f/f}$, *Dlg10* and *Dlg39* mice were fixed, embedded in paraffin, and sectioned as described above. Sections were subjected to TUNEL analysis using ApopTag® Plus Fluorescein In Situ Apoptosis Detection Kit (Chemicon) according to the manufacturer's instructions. Sections were counterstained with propidium iodide (PI) and viewed by confocal microscopy to visualize TUNEL positive and PI positive nuclei.

Immunofluorescence

Day E17.5 and P2 eyes from *Dlg-1*$^{+/+}$, *Dlg-1*$^{f/f}$, *Dlg10* or *Dlg39* mice were fixed, embedded in paraffin, and sectioned as described above. For protein detection on longitudinally oriented sections, sections were deparaffinized in xylenes and rehydrated using graded ethanols. Sections were boiled in 0.1M sodium citrate, pH 6.0, for 3 minutes at 60% power and were then trypsinized for 10 minutes at RT in a humidified chamber. For pERK, antigen retrieval was accomplished by boiling in 0.1M sodium citrate, pH 6.0, for 30 minutes in a rice cooker and then washed in 1X PBS. For transverse oriented sections, sections were trypsinized for one hour at RT. After antigen retrieval, all sections were blocked in 5% horse serum diluted in 1X PBS for 1 hour at RT. The blocking solution was removed and sections were incubated with primary antibodies diluted in blocking solution as described in Table 3 for 1 hour at RT up to overnight at 4°C. Sections were washed in 1X PBS and were incubated with the appropriate secondary: FITC conjugated horse anti-mouse (Vector Laboratories) or AlexaFluor 568 conjugated goat anti-rabbit (Molecular Probes). All secondary antibodies were diluted in 1X PBS. Sections were incubated for 1 hour at RT, then washed and viewed by confocal microscopy.

To visualize filamentous actin, cryosections of P2 *Dlg-1*$^{+/+}$, *Dlg-1*$^{f/f}$, *Dlg10* and *Dlg39* eyes were fixed in 4% PFA for 2 hours at 4°C and were then incubated in 10% and 20% sucrose for 1.5 hour each at 4°C and then overnight in 30% sucrose at 4°C. 10μm tissue cryosections were fixed in 4% PFA/0.25% Triton-X 100 for 10 minutes at RT, permeabilized with 0.2% Triton X-100 for 10 minutes at RT, and blocked O/N at 4°C with 5% horse serum. Sections were incubated with AlexaFluor 568-phalloidin (Molecular Probes) diluted 1:1000 in blocking solution for 1 hour at RT, washed and then viewed by confocal microscopy.

Acknowledgments

The authors thank Patricia Powers, Manorma John, Christopher Bartley, and Joe Warren of the University of Wisconsin Biotechnology Center's Transgenic Animal Facility for generating the *Dlg-1* conditional null mice. The authors also thank Paul Lambert and Sara Simonson for their participation in the generation of these mice, Lance Rodenkirch of the Keck Imaging Facility, Toshi Kinoshita of the Pathology Department Histology Core, Denis Lee and Susan Moran of McArdle Laboratory, and the McArdle Laboratory Histology Core for technical assistance with this project. The authors thank Paul Lambert for helpful discussions and his critical reading of the manuscript. I.F.Y. was supported by the NIH training grant GM07215. This work was supported by NIH grants EY09091 (AEG), CA98428 (AEG), CA14520 (AEG) and EY12995 (MLR).

REFERENCES

Bassnett S, Missey H, Vucemilo I. Molecular architecture of the lens fiber cell basal membrane complex. J Cell Sci. 1999; 112(Pt 13):2155–2165. [PubMed: 10362545]

Bilder D, Li M, Perrimon N. Cooperative regulation of cell polarity and growth by Drosophila tumor suppressors. Science. 2000; 289:113–116. [PubMed: 10884224]

Bilder D, Perrimon N. Localization of apical epithelial determinants by the basolateral PDZ protein Scribble. Nature. 2000; 403:676–680. [PubMed: 10688207]

Bilder D, Schober M, Perrimon N. Integrated activity of PDZ protein complexes regulates epithelial polarity. Nat Cell Biol. 2003; 5:53–58. [PubMed: 12510194]

Bossinger O, Klebes A, Segbert C, Theres C, Knust E. Zonula adherens formation in Caenorhabditis elegans requires dlg-1, the homologue of the Drosophila gene discs large. Dev Biol. 2001; 230:29–42. [PubMed: 11161560]

Brandt DT, Grosse R. Get to grips: steering local actin dynamics with IQGAPs. EMBO Rep. 2007; 8:1019–1023. [PubMed: 17972901]

Brumby A, Secombe J, Horsfield J, Coombe M, Amin N, Coates D, Saint R, Richardson H. A genetic screen for dominant modifiers of a cyclin E hypomorphic mutation identifies novel regulators of S-phase entry in Drosophila. Genetics. 2004; 168:227–251. [PubMed: 15454540]

Caruana G, Bernstein A. Craniofacial dysmorphogenesis including cleft palate in mice with an insertional mutation in the discs large gene. Mol Cell Biol. 2001; 21:1475–1483. [PubMed: 11238884]

Chen Y, Stump RJ, Lovicu FJ, McAvoy JW. Expression of Frizzleds and secreted frizzled-related proteins (Sfrps) during mammalian lens development. Int J Dev Biol. 2004; 48:867–877. [PubMed: 15558478]

Chen Y, Stump RJ, Lovicu FJ, McAvoy JW. A role for Wnt/planar cell polarity signaling during lens fiber cell differentiation? Semin Cell Dev Biol. 2006; 17:712–725. [PubMed: 17210263]

Chen Y, Stump RJ, Lovicu FJ, Shimono A, McAvoy JW. Wnt signaling is required for organization of the lens fiber cell cytoskeleton and development of lens three-dimensional architecture. Dev Biol. 2008; 324:161–176. [PubMed: 18824165]

Chepelinsky AB. The ocular lens fiber membrane specific protein MIP/Aquaporin 0. J Exp Zoolog A Comp Exp Biol. 2003; 300:41–46.

Chow RL, Roux GD, Roghani M, Palmer MA, Rifkin DB, Moscatelli DA, Lang RA. FGF suppresses apoptosis and induces differentiation of fibre cells in the mouse lens. Development. 1995; 121:4383–4393. [PubMed: 8575338]

de Iongh RU, Lovicu FJ, Overbeek PA, Schneider MD, Joya J, Hardeman ED, McAvoy JW. Requirement for TGFbeta receptor signaling during terminal lens fiber differentiation. Development. 2001; 128:3995–4010. [PubMed: 11641223]

Drees F, Pokutta S, Yamada S, Nelson WJ, Weis WI. Alpha-catenin is a molecular switch that binds E-cadherin-beta-catenin and regulates actin-filament assembly. Cell. 2005; 123:903–915. [PubMed: 16325583]

Faber SC, Robinson ML, Makarenkova HP, Lang RA. Bmp signaling is required for development of primary lens fiber cells. Development. 2002; 129:3727–3737. [PubMed: 12117821]

Ferreira-Cornwell MC, Veneziale RW, Grunwald GB, Menko AS. N-cadherin function is required for differentiation-dependent cytoskeletal reorganization in lens cells in vitro. Experimental Cell Research. 2000; 256:237–247. [PubMed: 10739670]

Firestein BL, Rongo C. DLG-1 is a MAGUK similar to SAP97 and is required for adherens junction formation. Mol Biol Cell. 2001; 12:3465–3475. [PubMed: 11694581]

Glaunsinger BA, Lee SS, Thomas M, Banks L, Javier R. Interactions of the PDZ-protein MAGI-1 with adenovirus E4-ORF1 and high-risk papillomavirus E6 oncoproteins. Oncogene. 2000; 19:5270–5280. [PubMed: 11077444]

Golestaneh N, Fan J, Fariss RN, Lo WK, Zelenka PS, Chepelinsky AB. Lens major intrinsic protein (MIP)/aquaporin 0 expression in rat lens epithelia explants requires fibroblast growth factor-induced ERK and JNK signaling. J Biol Chem. 2004; 279:31813–31822. [PubMed: 15145928]

Graw J. The crystallins: genes, proteins and diseases. Biol Chem. 1997; 378:1331–1348. [PubMed: 9426193]

Harris BZ, Lim WA. Mechanism and role of PDZ domains in signaling complex assembly. J Cell Sci. 2001; 114:3219–3231. [PubMed: 11591811]

Iizuka-Kogo A, Ishidao T, Akiyama T, Senda T. Abnormal development of urogenital organs in Dlgh1-deficient mice. Development. 2007; 134:1799–1807. [PubMed: 17435047]

Ishidate T, Matsumine A, Toyoshima K, Akiyama T. The APC-hDLG complex negatively regulates cell cycle progression from the G0/G1 to S phase. Oncogene. 2000; 19:365–372. [PubMed: 10656683]

Ishizaki Y, Jacobson MD, Raff MC. A role for caspases in lens fiber differentiation. J Cell Biol. 1998; 140:153–158. [PubMed: 9425163]

Iyengar L, Wang Q, Rasko JE, McAvoy JW, Lovicu FJ. Duration of ERK1/2 phosphorylation induced by FGF or ocular media determines lens cell fate. Differentiation. 2007; 75:662–668. [PubMed: 17381542]

Kiyono T, Hiraiwa A, Fujita M, Hayashi Y, Akiyama T, Ishibashi M. Binding of high-risk human papillomavirus E6 oncoproteins to the human homologue of the Drosophila discs large tumor suppressor protein. Proc Natl Acad Sci U S A. 1997; 94:11612–11616. [PubMed: 9326658]

Koppen M, Simske JS, Sims PA, Firestein BL, Hall DH, Radice AD, Rongo C, Hardin JD. Cooperative regulation of AJM-1 controls junctional integrity in Caenorhabditis elegans epithelia. Nat Cell Biol. 2001; 3:983–991. [PubMed: 11715019]

Lo WK, Shaw AP, Paulsen DF, Mills A. Spatiotemporal distribution of zonulae adherens and associated actin bundles in both epithelium and fiber cells during chicken lens development. Exp Eye Res. 2000; 71:45–55. [PubMed: 10880275]

Lovicu FJ, McAvoy JW. FGF-induced lens cell proliferation and differentiation is dependent on MAPK (ERK1/2) signalling. Development. 2001; 128:5075–5084. [PubMed: 11748143]

Lovicu FJ, McAvoy JW. Growth factor regulation of lens development. Dev Biol. 2005; 280:1–14. [PubMed: 15766743]

Lovicu FJ, Overbeek PA. Overlapping effects of different members of the FGF family on lens fiber differentiation in transgenic mice. Development. 1998; 125:3365–3377. [PubMed: 9693140]

Lyu J, Joo CK. Wnt signaling enhances FGF2-triggered lens fiber cell differentiation. Development. 2004; 131:1813–1824. [PubMed: 15084465]

Maddala R, Reneker LW, Pendurthi B, Rao PV. Rho GDP dissociation inhibitor-mediated disruption of Rho GTPase activity impairs lens fiber cell migration, elongation and survival. Dev Biol. 2008; 315:217–231. [PubMed: 18234179]

McAvoy JW, Chamberlain CG. Fibroblast growth factor (FGF) induces different responses in lens epithelial cells depending on its concentration. Development. 1989; 107:221–228. [PubMed: 2632221]

McMahon L, Legouis R, Vonesch JL, Labouesse M. Assembly of C. elegans apical junctions involves positioning and compaction by LET-413 and protein aggregation by the MAGUK protein DLG-1. J Cell Sci. 2001; 114:2265–2277. [PubMed: 11493666]

Morgenbesser SD, Williams BO, Jacks T, DePinho RA. p53-dependent apoptosis produced by Rb-deficiency in the developing mouse lens. Nature. 1994; 371:72–74. [PubMed: 8072529]

Nagasaka K, Nakagawa S, Yano T, Takizawa S, Matsumoto Y, Tsuruga T, Nakagawa K, Minaguchi T, Oda K, Hiraike-Wada O, Ooishi H, Yasugi T, Taketani Y. Human homolog of Drosophila tumor suppressor Scribble negatively regulates cell-cycle progression from G1 to S phase by localizing at the basolateral membrane in epithelial cells. Cancer Sci. 2006; 97:1217–1225. [PubMed: 16965391]

Naim E, Bernstein A, Bertram JF, Caruana G. Mutagenesis of the epithelial polarity gene, discs large 1, perturbs nephrogenesis in the developing mouse kidney. Kidney Int. 2005; 68:955–965. [PubMed: 16105026]

Nakagawa S, Huibregtse JM. Human scribble (Vartul) is targeted for ubiquitin-mediated degradation by the high-risk papillomavirus E6 proteins and the E6AP ubiquitin-protein ligase. Mol Cell Biol. 2000; 20:8244–8253. [PubMed: 11027293]

Nguyen MM, Nguyen ML, Caruana G, Bernstein A, Lambert PF, Griep AE. Requirement of PDZ-containing proteins for cell cycle regulation and differentiation in the mouse lens epithelium. Mol Cell Biol. 2003; 23:8970–8981. [PubMed: 14645510]

Nguyen MM, Potter SJ, Griep AE. Deregulated cell cycle control in lens epithelial cells by expression of inhibitors of tumor suppressor function. Mech Dev. 2002; 112:101–113. [PubMed: 11850182]

Nguyen MM, Rivera C, Griep AE. Localization of PDZ domain containing proteins Discs Large-1 and Scribble in the mouse eye. Mol Vis. 2005; 11:1183–1199. [PubMed: 16402019]

Nielsen PA, Baruch A, Shestopalov VI, Giepmans BN, Dunia I, Benedetti EL, Kumar NM. Lens connexins alpha3Cx46 and alpha8Cx50 interact with zonula occludens protein-1 (ZO-1). Mol Biol Cell. 2003; 14:2470–2481. [PubMed: 12808044]

Pan H, Griep AE. Altered cell cycle regulation in the lens of HPV-16 E6 or E7 transgenic mice: implications for tumor suppressor gene function in development. Genes Dev. 1994; 8:1285–1299. [PubMed: 7926731]

Piatigorsky J. Lens differentiation in vertebrates. A review of cellular and molecular features. Differentiation. 1981; 19:134–153. [PubMed: 7030840]

Pontoriero GF, Smith AN, Miller LA, Radice GL, West-Mays JA, Lang RA. Co-operative roles for E-cadherin and N-cadherin during lens vesicle separation and lens epithelial cell survival. Dev Biol. 2008

Ramos JW. The regulation of extracellular signal-regulated kinase (ERK) in mammalian cells. Int J Biochem Cell Biol. 2008; 40:2707–2719. [PubMed: 18562239]

Reuver SM, Garner CC. E-cadherin mediated cell adhesion recruits SAP97 into the cortical cytoskeleton. J Cell Sci. 1998; 111(Pt 8):1071–1080. [PubMed: 9512503]

Robinson ML, MacMillan-Crow LA, Thompson JA, Overbeek PA. Expression of a truncated FGF receptor results in defective lens development in transgenic mice. Development. 1995; 121:3959–3967. [PubMed: 8575296]

Robinson ML, Ohtaka-Maruyama C, Chan CC, Jamieson S, Dickson C, Overbeek PA, Chepelinsky AB. Disregulation of ocular morphogenesis by lens-specific expression of FGF-3/int-2 in transgenic mice. Dev Biol. 1998; 198:13–31. [PubMed: 9640329]

Segbert C, Johnson K, Theres C, van Furden D, Bossinger O. Molecular and functional analysis of apical junction formation in the gut epithelium of Caenorhabditis elegans. Dev Biol. 2004; 266:17–26. [PubMed: 14729475]

Simirskii VN, Wang Y, Duncan MK. Conditional deletion of beta1-integrin from the developing lens leads to loss of the lens epithelial phenotype. Dev Biol. 2007; 306:658–668. [PubMed: 17493607]

Stolen CM, Griep AE. Disruption of lens fiber cell differentiation and survival at multiple stages by region-specific expression of truncated FGF receptors. Dev Biol. 2000; 217:205–220. [PubMed: 10625547]

Thomas M, Laura R, Hepner K, Guccione E, Sawyers C, Lasky L, Banks L. Oncogenic human papillomavirus E6 proteins target the MAGI-2 and MAGI-3 proteins for degradation. Oncogene. 2002; 21:5088–5096. [PubMed: 12140759]

Walker JL, Zhang L, Zhou J, Woolkalis MJ, Menko AS. Role for alpha 6 integrin during lens development: Evidence for signaling through IGF-1R and ERK. Dev Dyn. 2002; 223:273–284. [PubMed: 11836791]

Woods DF, Bryant PJ. Molecular cloning of the lethal(1)discs large-1 oncogene of Drosophila. Dev Biol. 1989; 134:222–235. [PubMed: 2471660]

Woods DF, Hough C, Peel D, Callaini G, Bryant PJ. Dlg protein is required for junction structure, cell polarity, and proliferation control in Drosophila epithelia. J Cell Biol. 1996; 134:1469–1482. [PubMed: 8830775]

Yan Q, Liu JP, Li DW. Apoptosis in lens development and pathology. Differentiation. 2006; 74:195–211. [PubMed: 16759286]

Zampighi GA, Eskandari S, Kreman M. Epithelial organization of the mammalian lens. Exp Eye Res. 2000; 71:415–435. [PubMed: 10995562]

Zandy AJ, Lakhani S, Zheng T, Flavell RA, Bassnett S. Role of the executioner caspases during lens development. J Biol Chem. 2005; 280:30263–30272. [PubMed: 15994297]

Zelenka PS. Regulation of cell adhesion and migration in lens development. Int J Dev Biol. 2004; 48:857–865. [PubMed: 15558477]

Zhao H, Yang T, Madakashira BP, Thiels CA, Bechtle CA, Garcia CM, Zhang H, Yu K, Ornitz DM, Beebe DC, Robinson ML. Fibroblast growth factor receptor signaling is essential for lens fiber cell differentiation. Dev Biol. 2008; 318:276–288. [PubMed: 18455718]

Zhao H, Yang Y, Rizo CM, Overbeek PA, Robinson ML. Insertion of a Pax6 consensus binding site into the alphaA-crystallin promoter acts as a lens epithelial cell enhancer in transgenic mice. Invest Ophthalmol Vis Sci. 2004; 45:1930–1939. [PubMed: 15161860]

Zwaan J, Bryan PR Jr. Pearce TL. Interkinetic nuclear migration during the early stages of lens formation in the chicken embryo. J Embryol Exp Morphol. 1969; 21:71–83. [PubMed: 5765793]

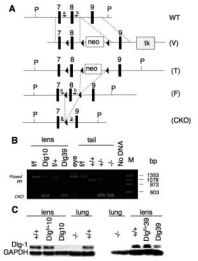

Figure 1. Generation of *Dlg-1* conditional mutant mice

A: Diagram showing the targeting vector and steps to generate the *Dlg-1* conditional knockout. Shown is a portion of the WT allele highlighting exons 7-9 and arrows to indicate the location for PCR primers a and b (see Table 1, PCR primer combination 1, primer a=Dlg 5′ forward and primer b=Dlg8R reverse) for genotyping. The targeting vector (V) is shown, indicating lox P sites (arrowheads), placement of the positive selection neomycin marker (neo) and the negative selection Herpes simplex virus thymidine kinase (tk) marker after exon 9. Shown is the targeted allele (T) carried by the correctly targeted ES cell clones that were used to generate chimeras. Shown is the floxed allele (F), which was generated after mating to *EIIAcre* mice to remove the neo marker is shown. Arrows indicate locations for PCR primers a and b (See Table 1, primer combination 1), which were used for routine genotyping of the mice. Finally, the conditional knockout (CKO) allele is shown, which results from lens specific cre induced deletion of exon 8. Arrows indicate locations of PCR primers a and c (see Table 1, PCR primer combination 2, primer c=Dlg 3′ reverse) which were used to verify that exon 8 had been deleted specifically in lens DNA. **B:** Lens-specific cre mediated deletion of exon 8. PCR primers a and c were used to amplify DNA fragments from lens and tail samples of mice with the indicated genotypes. The band representing the wild type allele is 1058 bp while the band representing the floxed alleled is 1273 bp. The 380 bp band representing the deleted allele is observed when PCR was carried out on DNA from Dlg-1 mutant lenses, and on tail samples from mice heterozygous or homozygous for the germline null allele. **C:** Western blot analysis from whole lens (*Dlg10*) or fiber extracts (*Dlg39*) from P2 mice of the indicated genotypes showing reduced levels of Dlg-1 in lenses from CKO mice as compared to a GAPDH loading control. To demonstrate the specificity of the antibody, protein extracts from *Dlg-1*$^{+/+}$ and *Dlg-1*$^{-/-}$ lung samples were blotted at the same time.

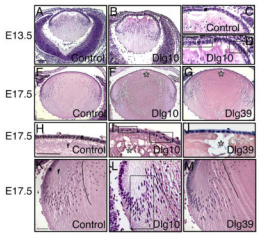

Figure 2. Morphological defects in lenses from *Dlg-1* mutant embryos

Longitudinally oriented, paraffin embedded samples from E13.5 (A-D) and E17.5 (E-M) control (A,C,E,H,K), *Dlg10* (B,D,F,I,L) and *Dlg39* (I,M) mice were sectioned and the sections then stained hematoxylin and eosin. Shown are representative sections. **A-B:** Eyes from E13.5 control (A) and *Dlg10* (B) embryos. **C-D:** Higher magnification view of the epithelium from E13.5 control (C) and *Dlg10* (D) mice showing the disorganized epithelium in the lens of the *Dlg10* mice. Boxes indicate regions of multilayering. **E-G:** Lenses from E17.5 control (E), *Dlg10* (F) and *Dlg39* (G) embryos. Lenses of the *Dlg10* (F) and *Dlg39* (G) mice showed defects in anterior and posterior suture formation (asterisk). **H-J:** Higher magnification view of epithelium from control (H), *Dlg10* (I) and *Dlg39* (J) E17.5 embryos highlighting defects in the organization of the epithelial cells specifically in the epithelium of the *Dlg10* mice (boxes). **K-M:** Higher magnification view of transition zones of lenses from control (K), *Dlg10* (L) and *Dlg39* (M) mice highlighting defects in the normal “C” shape of the fiber cells (lines) and positioning of fiber cell nuclei in the bow region of the *Dlg10* mice (box). e=epithelium, f=fibers. Scale bar=100μm for A, B, E-G and 50 μm for C, D, H-M.

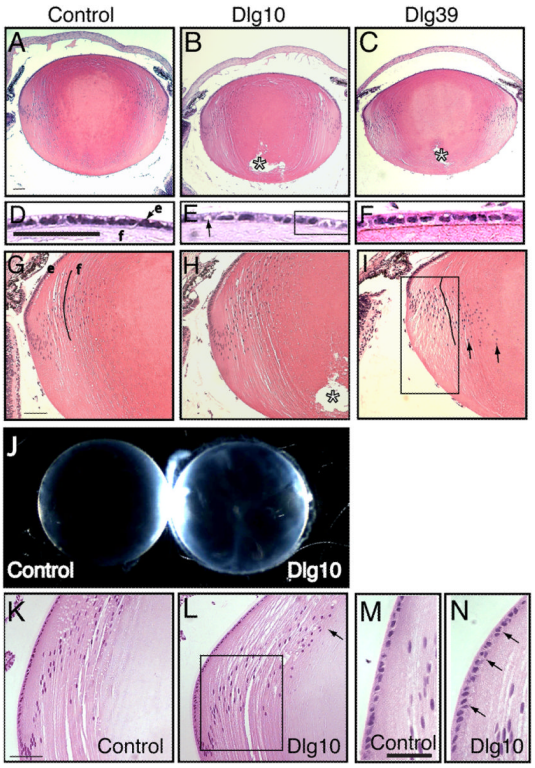

Figure 3. Morphological defects and cataract formation in lenses from postnatal *Dlg-1* mutant mice

Longitudinally oriented, paraffin embedded eye sections from control, *Dlg10* and *Dlg39* postnatal mice were stained with hematoxylin and eosin. Shown are representative stained sections. Whole lenses from control and *Dlg10* mice were also examined for cataract formation. **A-C:** Low magnification view of lenses from control (A), *Dlg10* (B) and *Dlg39* (C) P2 mice. Posterior suture defects are readily apparent in the lenses of *Dlg10* and *Dlg39* mice (asterisk). **D-F:** Higher magnification view of the epithelium from control (D), *Dlg10* (E) and *Dlg39* (F) P2 mice. The epithelium from the lenses of the *Dlg10* mice show irregularities in the organization and appearance of the nuclei, vacuoles (arrow) and regions of loosely packed cells lacking nuclei (box). **G-I**: Higher magnification view of the transition zone in lenses of the control, *Dlg10* and *Dlg39* P2 mice. In (I) the eosin staining was weaker, suggesting defects in the packing of the fibers in *Dlg39* mice (I, Box). Also, nuclei did not bow upwards, but instead extended into the posterior region of the lens (arrows). Additionally, fibers did not maintain their normal “C” shape (lines). e=epithelium, f=fibers. **J:** Whole lenses from control and *Dlg10* P24 mice were viewed under a dissecting microscope. Lenses from *Dlg10* mice exhibited cataracts. **K-L:** View of the bow region from control (K) and *Dlg10* (L) P24 mice. Compared to the tight bow region of the control lenses, the bow region in the lenses of the *Dlg10* mice was broader and many nuclei had failed to migrate anteriorly (box). Denucleation appeared delayed, as the cortical fiber region was expanded and rounded nuclei were observed encroaching on the center of the lens (arrow). **M-N:** High magnification of the epithelium in the bow region of control (M) and *Dlg10* (N) mice. Compared to controls, the nuclei in the epithelium of the *Dlg10* lenses were disorganized, sometimes being multilayered, and irregularly shaped (arrows). Scale bar=100μm for A-C, G-I, K-L and 50μm for D-F, M-N.

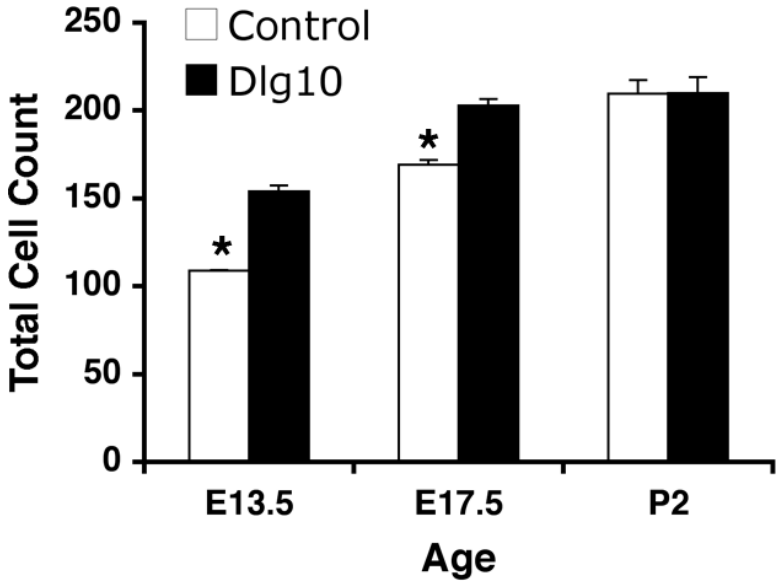

Figure 4. Increased total cell number in the lens epithelium of *Dlg10* embryos

The total number of cells in the lens epithelium of control and *Dlg10* E13.5, E17.5 and P2 mice were counted on hematoxylin and eosin paraffin embedded section from the center of the lens. The total number of cells in the epithelium of *Dlg10* mice at E13.5 and E17.5 was greater than in controls ($p<0.05$) while at P2 the total number of cells in epithelium of mutant and control mice were not different. At least 3 animals per genotype per age and 2 slides per animal per age were used.

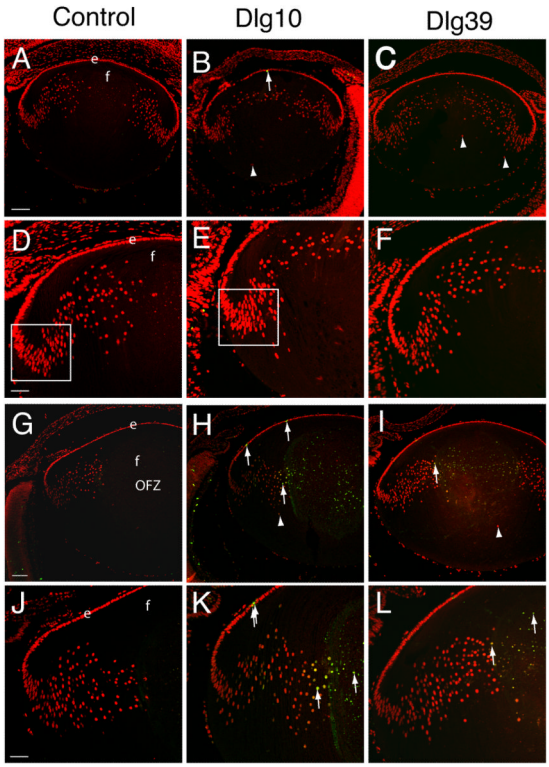

Figure 5. Induction of apoptosis in lenses of postnatal *Dlg-1* mutant mice

Longitudinally oriented, paraffin embedded eyes sections from E17.5 (A-F) and P2 (G-L) control (A,D,G,J), *Dlg10* (B,E,H,K) and *Dlg39* (C,F,I,L) mice were subjected to fluorescein-TUNEL assay (green) and counterstained with propidium iodide (PI, red). **A-C:** Low magnification view of lenses from E17.5 control (A), *Dlg10* (B) and *Dlg39* (C) mice. At E17.5, no apoptotic cells were observed in lenses from control, *Dlg10* or *Dlg39* mice except for the occasional cell in the epithelium (B, arrow). Shown are defects in nuclear organization in the fiber cell compartment of *Dlg10* and *Dlg39* mice (arrowheads). **D-F**: Higher magnification view of lenses in (A-C). Box indicates the high density of nuclei often observed in this region of lenses from the *Dlg10* mice. **G-I:** Low magnification view of lenses from P2 control (G), *Dlg10* (H) and *Dlg39* (I) mice. Apoptotic cells are readily detected in the center of the lenses from *Dlg10* and *Dlg39* mice (arrows) and nuclei are also mislocalized (arrowheads). Lenses from *Dlg10* mice also showed an increase in the number of apoptotic cells in the epithelium as compared to controls. **J-L:** Higher magnification views of lenses in (G-I) highlighting apoptotic nuclei in the cortical fibers and center of the lenses (arrows) from *Dlg10* and *Dlg39* mice and in the epithelium of the *Dlg10* mice. e=epithelium, f=fibers. Scale bar=100 μm for A-C, G-I and 50μm for D-F, J-L.

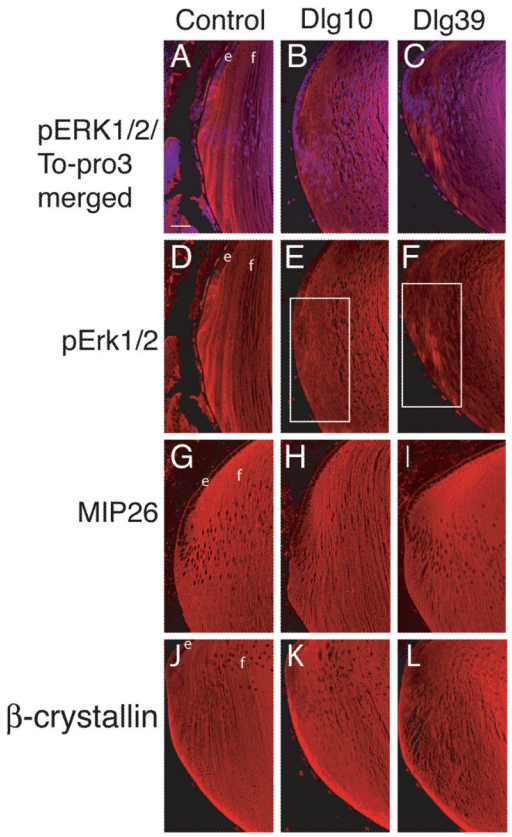

Figure 6. Reduced accumulation of pERK in transition zone of lenses from *Dlg10* and *Dlg39* mice

Longitudinally oriented, paraffin embedded eye sections from P2 control (A,D,G,J), *Dlg10* (B,E,H,K) and *Dlg39* (C,F,I,L) mice were subjected to immunoflourescence analysis for three markers of fiber cell differentiation. **A-C:** Merged images of control (A), *Dlg10* (B) and *Dlg39* (C) lenses stained with To-PRO3 (blue nuclei) and an anti-pERK antibody (red). **D-F:** Unmerged images corresponding to A-C show anti-pERK staining (red) only. White boxes show the patchy and reduced accumulation of pERK staining in the transition zone in *Dlg10* (E) and *Dlg39* (F) mice. **G-H:** Sections from control (G), *Dlg10* (H) and *Dlg39* (I) mice were immunostained with anti-MIP26 antibodies. The pattern of MIP26 immunostaining was not altered in lenses of *Dlg10* or *Dlg39* mice as compared to controls. **J-L:** Sections of control (J), *Dlg10* (K) and *Dlg39* (L) mice were immunostained with anti-β crystallin antibodies. The pattern of β-crystallin immunostaining was not altered in lenses of *Dlg10* or *Dlg39* mice as compared to controls. e=epithelium, f=fibers. Scale bar=50μm.

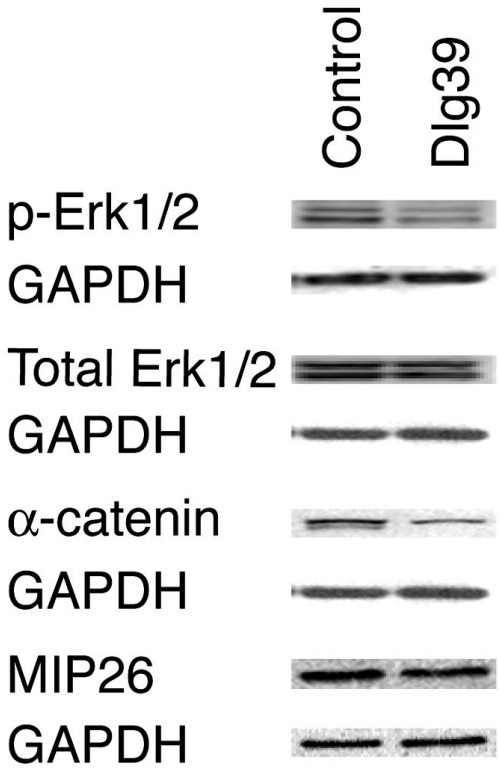

Figure 7. Reduced levels of pERK1/2, α-catenin and MIP26 in *Dlg39* fiber cells by immunoblot analysis

100μg of RIPA protein lysates from the fiber cells of control and *Dlg39* P2 mice was immunoblotted for pERK1/2, total ERK1/2, α-catenin, MIP26 and GAPDH, which served as a loading control, as described in Experimental Procedures and Table 2. Total pERK1/2 levels were reduced in *Dlg39* mutants while ERK1/2 levels appeared unchanged. Total α-catenin and MIP26 levels were also reduced in fiber cell extracts from *Dlg39* mice as compared to extracts from control mice. Two pools each of control and *Dlg39* lens fiber cells (consisting of 18-21 lenses in each pool) were analyzed.

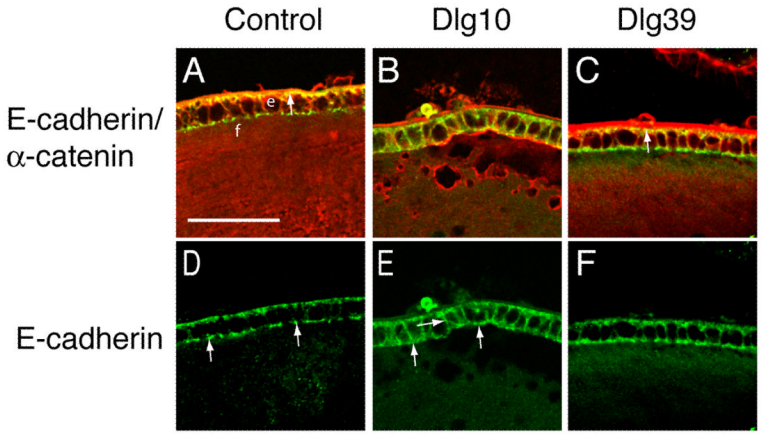

Figure 8. Mislocalization of E-cadherin in the epithelium of *Dlg10* mice

Longitudinally oriented, paraffin embedded eye sections from control (A,D), *Dlg10* (B,E) and *Dlg39* (C,F) E17.5 embryos were subjected to double immunofluorescence with anti-E-cadherin (green) and anti-α-catenin (red) antibodies. Shown are representative images of a portion of the central epithelium (e) and underlying fiber cells (f). **A, D:** Merged image (A) of E-cadherin and α-catenin immunostaining on control lenses showing overlap (yellow) in staining along the basal surface of the epithelial cells. The unmerged E-cadherin only image (D) shows the punctate staining for E-cadherin along the apical membrane (arrows) and weak staining along the lateral membranes. **B, E:** Merged image of E-cadherin and α-catenin staining on lenses of *Dlg10* embryos (B) showing a lack of overlap along the basal surface of the epithelial cells and ectopic overlap along basal and lateral membranes. The unmerged E-cadherin only image (E) shows diffuse staining on the apical surface (arrows), and the ectopic staining on the lateral surfaces. (arrows). **C, F:** Merged image (C) showing overlap in E-cadherin and α-catenin staining in lenses from *Dlg39* mice. The pattern of co-localization of E-cadherin and α-catenin is the same as the control, as is the distribution of E-cadherin along the membrane surfaces (F). The intense red staining of the lens capsule in (C) is artifactual, as it was observed in sections stained with secondary antibody only. e=epithelium, f=fibers. Scale bar=50μm.

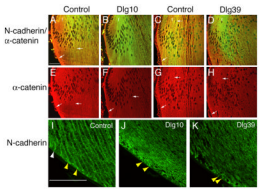

Figure 9. Disruption of N-cadherin and α-catenin co-localization in the fiber cell compartment of *Dlg-1* mutant mice

Longitudinally oriented, paraffin embedded eye sections from control (A,C,E,G,I), *Dlg10* (B,F,J) and *Dlg39* (D,H,K) E17.5 embryos (A,B,E,F) and P2 (C,D,G,H, I, J, K) mice were subjected to double immunofluorescence with anti-N-cadherin (green) and anti-α-catenin (red) antibodies. Shown are representative images of the transition zones (A-H) and posterior (I-L) regions of the lenses. **A, C**: Merged image of N-cadherin and α-catenin immunostaining in lenses from control E17.5 (A) and P2 (C) mice showing co-localization (yellow) along the lateral membranes and posterior tips of fiber cells (arrows). **B, D**: Merged image of N-cadherin and α-catenin immunostaining in lenses from *Dlg10* (B) and *Dlg39* (D) mice showing reduced co-localization and reduced α-catenin staining. **E, G:** Unmerged images showing strong α-catenin staining along the membranes and posterior tips in control E17.5 (E) and P2 (G) lenses (arrows). **F, H:** Unmerged images showing reduced α-catenin staining in lenses of *Dlg10* (F) and *Dlg39* (H) mice (arrows). **I**: Immunostaining for N-cadherin posterior to the transition zone in lenses from control E17.5 embryos. Note the reorientation of the basal tips of the fiber cells along the capsule from concave to convex (white arrowheads vs. yellow arrowheads) and the highly ordered arrangement of the fiber cells. **J, K**: Immunostaining for N-cadherin posterior to the transition zone in lenses from *Dlg10* (J) and *Dlg39* (K) P2 lenses. Note that the basal tips of the fibers are randomly organized with respect to the capsule (yellow arrowheads). Also note the disruption of fiber cell organization. f=fibers. Scale bar=50μm.

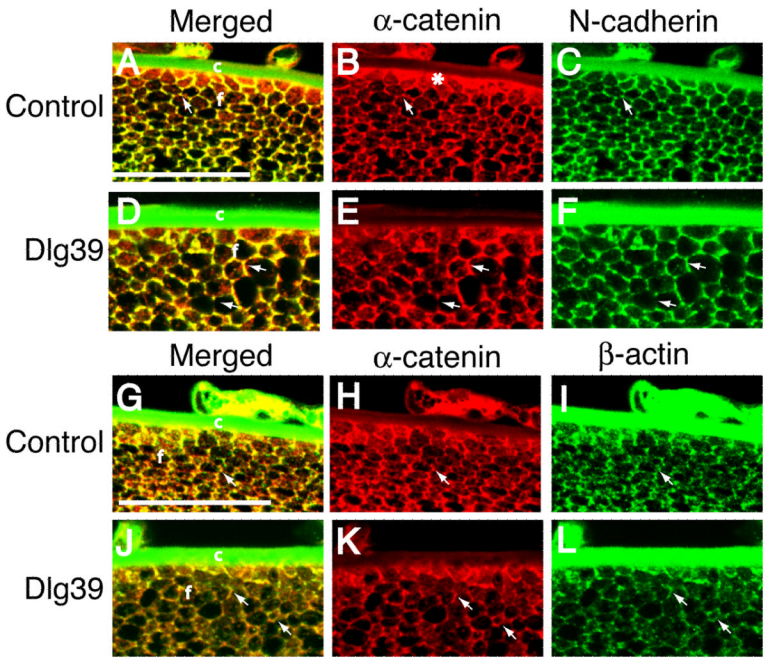

Figure 10. Disrupted fiber cell shape and co-localization of N-cadherin, α-catenin and β-actin in the fiber cells of *Dlg39* mice

Transversely oriented, paraffin embedded eye sections from control (A-C, G-I) and *Dlg39* (D-F, J-L) mice were subjected to immunostained with anti-α-catenin (red) and anti-N cadherin (green) antibodies (A-F) or anti-α-catenin (red) and anti-β-actin (green) antibodies (G-L). Shown are representative high resolution images taken from the region just posterior to the transition zone. **A-C:** Merged and unmerged images of α-catenin (red) and N-cadherin (green) staining in control lenses. (A) Shown is the punctate, overlap in α-catenin and N-cadherin staining (yellow) at the vertices of the hexagonally shaped fiber cells in the lenses of the control mice (arrow). (B, C) Unmerged images showing the staining for α-catenin (red) on all the membranes and staining for N-cadherin (green) primarily at the vertices and short sides of the fiber cells. Also shown is the concentration of α-catenin at the basal tips of the fiber cells (asterisk in B). The green staining of the lens capsule is artifactual, as it was observed in sections stained with secondary antibody only. **D-F:** Merged and unmerged images of α-catenin and N-cadherin staining in *Dlg39* lenses. (D) Shown is the disrupted, nonuniform shape of the fiber cells. Overlap in staining for α-catenin and N-cadherin is sometimes observed along the entire length of the sides of the fiber cells whereas in other cells, overlap is absent (see arrows). (E, F) Unmerged images showing the irregularities in the staining for α-catenin and N-cadherin (arrows). Also notice the accumulation of α-catenin at the basal tips is reduced in the lenses of the *Dlg39* mice. **G-I:** Merged and unmerged images of α-catenin (red) and β-actin (green) staining in control lenses. (G) Shown is the concentrated, punctate, overlap in α-catenin and β-actin staining (yellow) at the vertices of the hexagonally shaped fiber cells (arrow). (H, I) Unmerged images showing the staining for α-catenin (red) on all the membranes and for β-actin (green) concentrated at the vertices of the fiber cells. Also shown is the concentration of α-catenin at the basal tips of the fiber cells (asterisk in H). **J-L:** Merged and unmerged images of α-catenin and β-actin staining in *Dlg39* lenses. (J) Shown is the disrupted, nonuniform shape of the fiber cells. Overlap in staining for α-catenin and β-actin at the vertices is reduced. Some membranes stained for both α-catenin and β-actin in a mainly non-overlapping pattern (arrows). (K, L) Unmerged images showing the irregularities in the staining for α-catenin and staining for β-actin (arrows). c=lens capsule; f=fiber cell compartment. Scale bar=50 μm.

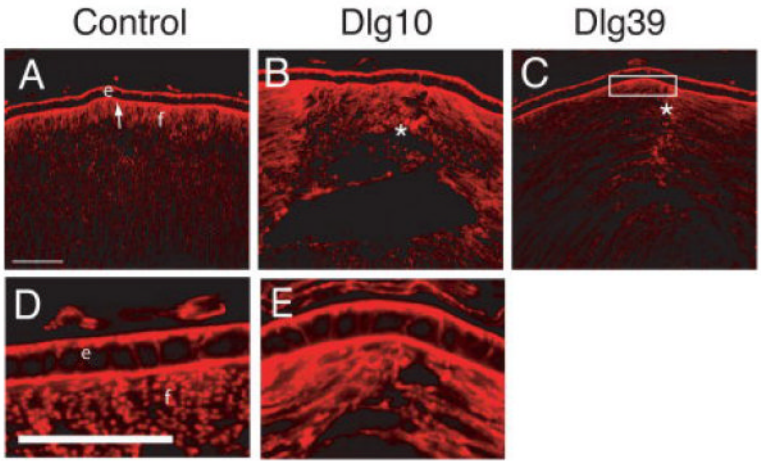

Figure 11. Disrupted actin organization in lenses of *Dlg-1* mutant mice

Longitudinally oriented, cryosections of eyes from control (A, D), *Dlg10* (B, E) and *Dlg39* (C) P2 mice were stained with phalloidin to visualize filamentous actin. Shown are representative sections. **A, D:** In controls, actin is concentrated at the basal and apical surfaces of epithelial cells. At the apical ends of the fiber cells actin has a uniform pattern and is highly concentrated. **B, E:** In lenses from *Dlg10* mice, actin accumulation in the epithelium appeared normal. However, in the fibers actin organization was disrupted where anterior sutures normally form (asterisk). **C:** In lenses from *Dlg39* mice, actin accumulation was decreased in the apical ends of the fiber cells (box) and actin organization was nonuniform, especially where the suture forms. e=epithelium, f=fibers. Scale bars=50μm.

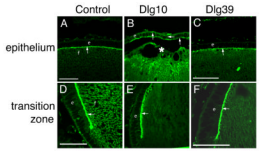

Figure 12. Mislocalization of the apical polarity marker, ZO-1, in the central epithelium of lenses of *Dlg10* embryos

Longitudinally oriented, paraffin embedded eye sections from E17.5 control (A,D), *Dlg10* (B,E) and *Dlg39* (C,F) embryos were immunostained with anti-ZO-1 antibodies. **A:** Immunostained control lenses (A), showed ZO-1 localized exclusively to the apical membrane of the cells in the central epithelium and apical tips of the fiber cells (arrow). Immunostained lenses of *Dlg10* embryos (B) showed ZO-1 on all membranes of central epithelial cells and showed discontinuous staining on the apical membrane (arrows). **C:** Immunostained lenses of *Dlg39* embryos showed staining in the epithelium that was indistinguishable from that of control lenses. **D-F:** In the transition zone, immunostaining showed localization of ZO-1 at the apical surface of epithelial cells in lenses from control mice (D) as well as in lenses from *Dlg10* (E) and *Dlg39* (F) mice (arrows). e=epithelium, f=fibers, asterisk=fiber cell elongation defect. Scale bars=50μm.

Table1

PCR Primer Combinations

Combination	Primer Names	Sequence	Expected Size	Identifies
1	Dlg5′ Forward	5′ CAT CAT GGT TGA AGT GCT CTG GGC 3′	Wt=540bp Floxed=753bp	Dlg-1 Wt and Floxed Alleles
	DlgI8R Reverse	5′AAA TGT GGC CTG AGG ATC TAC CTC CG 3′		
2	Dlg5′ Forward	5′ CAT CAT GGT TGA AGT GCT CTG GGC 3′	Wt=1058bp Floxed=1273bp CKO=380bp	Wt, CKO, and Floxed allele
	Dlg3′ Reverse	5′ GGA AGG AAA CTC ACG GAT GGT CC 3′		
3	Pr4	5′ GCA TTC CAG CTG CTG ACG GT 3′	Cre Band= 577bp	Cre transgene
	CreAS	5′ CAG CCC GGA CCG ACG ATG AAG 3′		

Table2

Primary Antibodies for Western Blotting

Western Primary Antibodies	Company	Dilution
Mouse anti-Dlg-1	Stressgen, BD Biosciences	1:1000
Mouse anti- α Catenin	Zymed	1:1000
Rabbit anti-Active ERK (pERK)	Cell Signaling	1:1000
Rabbit anti-ERK	Promega	1:1000
Rabbit anti-MIP26	Alpha Diagnostics	1:2500
Mouse anti-GAPDH	Chemicon	1:10,000

Table3

Primary Antibodies for Immunofluorescence

Immunofluorescence Antibodies	Company	Dilution
Rabbit anti-Active ERK (pERK)	Cell Signaling	1:50
Rabbit anti-MIP26	Alpha Diagnostics	1:250
Rabbit anti-β Crystallin	Gift	
TO-PRO 3	Invitrogen	1:500
Mouse anti-b-actin	Sigma	1:100
Mouse anti-E-Cadherin	BD Biosciences	1:100
Rabbit anti-α-Catenin	Sigma	1:250
Mouse anti-N-Cadherin	BD Biosciences	1:100
Mouse anti-ZO-1	Zymed Laboratories	20μg/ml